Design and Simulation of an Enhanced Bandwidth Microstrip Antenna Using Metamaterial

Mustafa H. Abbas[#1], Jabir S. Aziz[*2]

[#] *Electronics and communication engineering department, College of Engineering, Al-Nahrain University*
Baghdad-Iraq

[*] *Electronics and communication engineering department, College of Engineering, Al-Nahrain University*
Baghdad-Iraq

Abstract— **The remarkable broadband characteristics of the ultra-wideband (UWB) antennas continue to acquire the attention of a large number of researchers and developers in wireless communication area around the world during the past years. For that purpose, a metamaterial microstrip antenna is proposed to cover the IEEE 802.15.4a (3.1-10.6 GHz) UWB designation and even extend to more than that, it almost reaches the 18 GHz. A huge bandwidth enhancement can be achieved in the UWB antenna by adding different shapes of cells called metamaterial. The presented design integrates two types of metamaterial cells located on the patch and the groundside, and microstrip feed line.**

Keywords— **Ultra-wideband, Metamaterial, Negative Refractive Index, Double Negative Medium, Unit Cell.**

I. INTRODUCTION

Ultra-Wideband Radio (UWB) is an insurgent approach to wireless communication when the pulse-based waveforms can be transmitted and received compressed in time instead of compressed it in frequency as a sinusoidal waveform. This approach allows transmitting over a wide range of frequencies. On this basis, a very low power spectral density (PSD) can be clearly received. Therefore, it is obvious that this approach is opposite to the conventional transmission agreements over a very narrowband frequency, typical of the standard narrowband systems for example 802.11a, b, and Bluetooth [1].

Any communication technology operates with bandwidth of 500 MHz or more which equates to 25% of the operating center frequency can be considered as an Ultra-Wideband technology. On the other hand, most narrowband systems are transmitted at high power levels and seize less than 10% bandwidth of its center frequency [2].

High data rates are possible for communication applications due to the large number of pulses that can be created in short time duration. And because of its low power spectral density, UWB is being used in military applications that require low probability of detection. In addition, the UWB technology can be used in radar and imaging technologies, where the ability to resolve multipath delay is in the nanosecond range, allowing for finer resolution whether it be from a target or from an image. After recognizing the potential advantages of UWB, FCC developed a report to allow UWB as a communications and imaging technology [3].

In spite of the many advantages of the Microstrip antenna like low cost of production, slim profile, ease of fabrication, lightweight, and the compatibility with MMIC (i.e. Monolithic Microwave Integrated Circuit) design, the microstrip antenna is suffering from natural limitations such as the narrow bandwidth, low efficiency, and low power capacity. The main challenge in UWB antenna design is achieving the wide impedance bandwidth while still maintaining high radiation efficiency [4].

Many enhancement techniques were found to increase the bandwidth of MSA such as the stacked antenna technique, the planner coupled antenna and the slotted antenna. Another technique was invented to solve the narrow band problem, which is the metamaterial antenna.

Electromagnetic metamaterials (MTMs) are synthetic materials prepared to offer properties that cannot be obtained easily in nature. These materials achieve their properties from their structure by using the insertion of small inhomogeneous materials to endorse the consequence of the macroscopic behaviour [5].

The micro system technologies and nanotechnologies have enabled the penetration in many different areas of science and technology. In addition, they also present the functions beyond nature. It is used in electromagnetic and optical applications by enabling its material's structure. Photonic crystals are considered as one of the best examples of original electromagnetic structures and the negative refractive index metamaterials, popularly known as "left-handed" materials [5]. Negative refractive index metamaterials (NRI-M) are artificial composites, characterized by subwavelength features and negative effective value of refractive index.

Permittivity, ε and permeability μ are the main parameters, which describe the propagation of EM waves in a medium. Permittivity ε describes the relation between electric field strength E and electric displacement D. While the Permeability μ describes the relation between magnetic field strength H and magnetic flux density B. medium with simultaneously negative permittivity and negative permeability ($\varepsilon_r < 0$, $\mu_r < 0$) is called a Double Negative Medium (DNG) or Left-handed (LH) material. And the refractive index is negative [6]:

$$n = \pm \sqrt{\frac{\varepsilon \mu}{\varepsilon_0 \mu_0}} = \pm \sqrt{\varepsilon_r \mu_r} \qquad \ldots (1)$$

The idea of metamaterials began with Vaselago, and evolved by Pendry that proposed a different type of array composed of conducting Split-Ring Resonator (SRR) that could have negative permeability over certain range of frequencies [7]. After that, Smith et al inspired by Pendry's work proposed an artificial effectively homogeneous metamaterial structure with simultaneous negative permittivity ε and negative permeability μ [8]. The structure essentially was a composite of two of the Pendry's structures (TW and SRR) as shown in Fig. 1.

Figure 1 First True "backward-wave media (BW media) Proposed by Smith et al. composed of Thin Wire (TW) and Split - Ring Resonators (SRR). (A) 1D media. (B) 2D media

II. Reference Microstrip Antenna

The geometry of microstrip antenna is shown in Fig. 2. The mechanism of the operation of each parameter in the antenna should be studied in order to determine its initial value. In general, the microstrip antennas have the capability to support the wideband range of frequency in the subject of FCC federation with a finite ground plane in comparison with the band of complete ground plane.
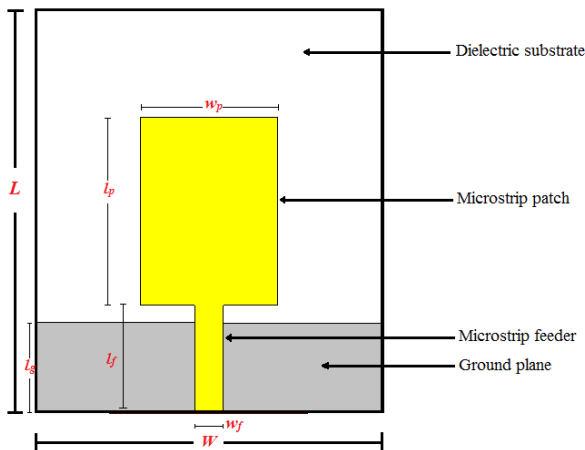

Figure 2 The configuration of the UWB microstrip antenna showing the necessary antenna parameters.

Fig. 3 shows the geometry of the UWB monopole disk antenna. The antenna is to be modelled using an FR4 substrate with thickness of 1.6 mm and relative permittivity of 4.3. On the front surface of the substrate, a rectangular radiating patch with initial dimensions of 27.5 mm × 32 mm, has been etched. For design convenience, a 50 Ohm microstrip line printed on the radiator side of the substrate feeds the proposed antenna. The feed line width is of about 2.3 mm, and is symmetrically located with respect to both

the radiating element and the ground plane. On the other side of the substrate, a conducting ground plane of 27.5 mm × 8 mm is placed and Table 1 shows the dimensions of the antenna.

Table 1: Reference Antenna Parameter and Dimensions.

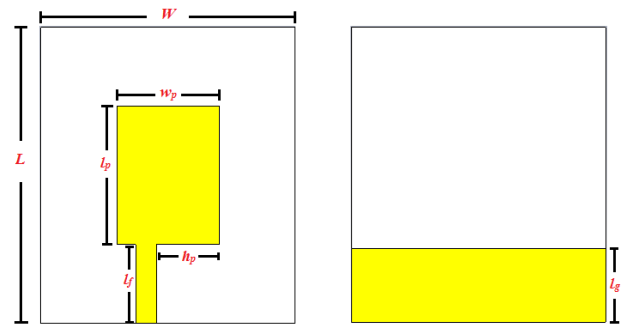| Parameter	Description	Value (mm)
l_g	Length of ground	8
l_f	Length of feed line	8.5
w_f	Width of feed line	2.26
l_p	Length of patch	15
w_p	Width of patch	11
h_p	Feeder position	7.1

Figure 3 The proposed reference antenna.

A- The Effect of the Patch Length on the Bandwidth

The return loss responses of the modelled antenna, shown in Fig. 4, have been carried out for different sizes of the patch length (l_p). It is clearly shown that the variation of the length has an effect on the lower frequency f_L position only.
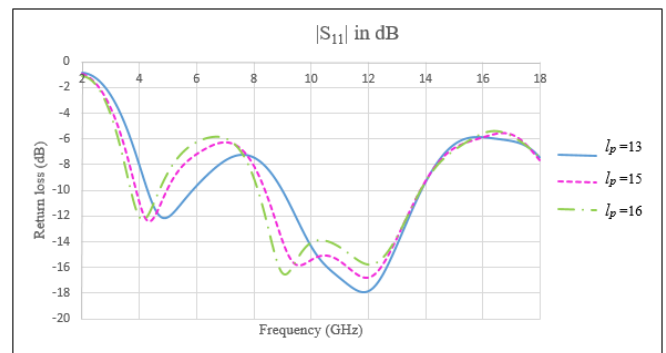

Figure 4 The return loss responses of antenna structure with l_p as a variable parameter.

From Fig. 4, it is obvious that changing the length of the patch has effect on the lower frequency only. Also it shows that increasing the length of patch (l_p) will increase the bandwidth.

B- The Effect of the patch width on the Bandwidth

The return loss responses of the modelled antenna shown in Fig. 5 represents the effect of changing the width of patch (w_p) on the frequency range.
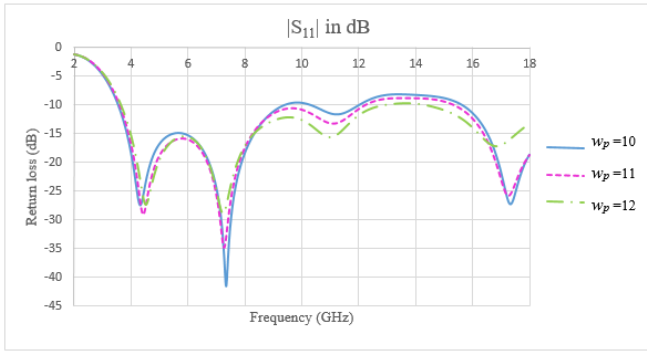
Figure 5 The return loss responses of antenna structure with w_p as a variable parameter.

It is shown from Fig. 5 that the variation of the width has an effect on the higher frequency f_H position only. In addition, it is obvious that increasing the width of the patch will guarantee the increasing of the bandwidth.

C- The Effect of the Ground Length on the Bandwidth

A sweep of the parameter (l_g) has been taken as shown in Fig. 6 that represents samples of the return loss responses of the sweep of the ground plane l_g. It is clearly shown that the variation of the ground plane has little effect on the lower frequency f_L position, while its effect on the higher frequencies becomes clearer.

Figure 6 The return loss responses of antenna structure with l_g as a variable parameter

From Fig. 6, it can be seen that the variation of the length of ground will affect the bandwidth of the design, as it will change the number of pass band frequencies and the high and low cutoff frequencies. In addition, it can be noticed that when the length of ground is approximately the same as the length of the feed line we can get the broadest bandwidth while increasing the difference between the feed line and ground length which will decrease the bandwidth.

D- The Effect of the Feeder Position on the Bandwidth

Fig. 7 shows the return loss responses of the modelled antenna after changing the position of the feeder (h_p). It is clearly shown that the variation of the position has little effect on the lower frequency f_L position and enhances the bandwidth in higher frequency f_H.
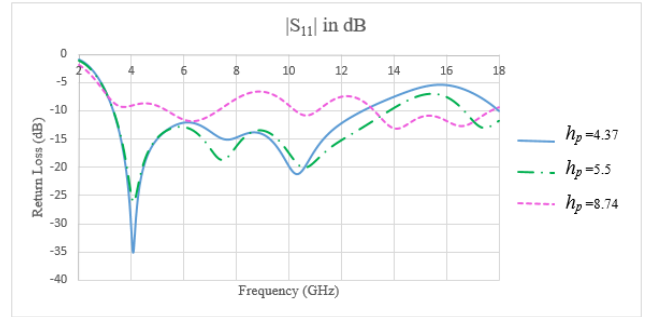

Figure 7 The return loss responses of antenna structure with h_p as a parameter.

E- The Effect of the Feed Line Length on the Bandwidth

The return loss responses of the modelled antenna, shown in Fig. 8, have been carried out for different lengths of the feed line (l_f). It is obvious that the variation of the feed line length has little effect on the lower frequency f_L position, and improves the BW for the range of frequencies 8-12 GHz.
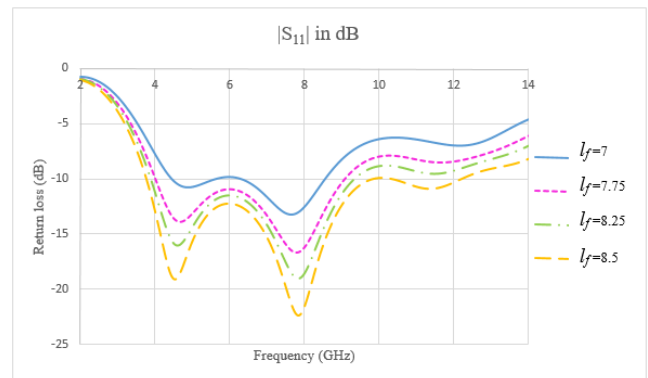

Figure 8 The return loss responses of antenna structure with l_f as a parameter.

F- The Effect of the Feed Line Width on the Bandwidth

The return loss responses of the modelled antenna, shown in Fig. 9, have been carried out for different width of the feed line (w_f). It shows the small improvement in the higher frequency f_H in the range (10-12 GHz).
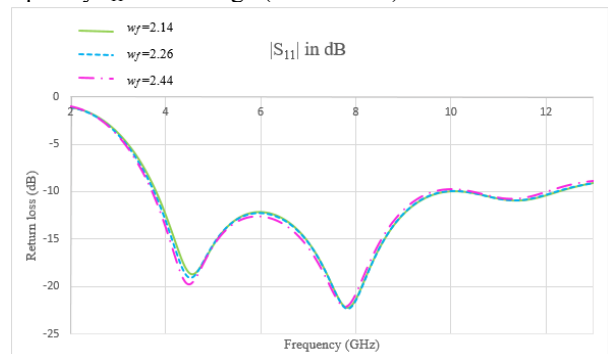

Figure 9 The return loss responses of antenna structure with w_f as a parameter.

401

III. IMPROVING ANTENNA BANDWIDTH USING METAMATERIAL CELL TYPE I

First type of metamaterial unit cell will be added to the substrate in the backside of the antenna. The design will be a matrix of 7×6 arrays of metamaterial cells. Cell geometry and parameters information are described as shown in Fig. 10.
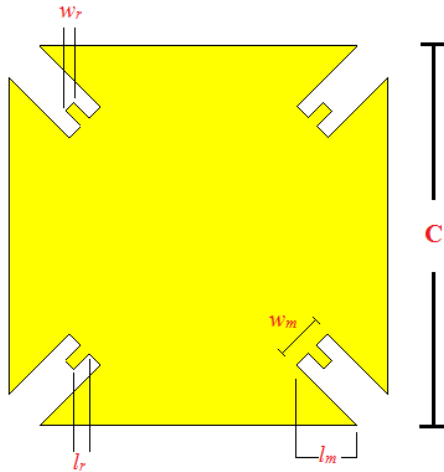

Figure 10 The geometry and parameters of metamaterial unit cell type I

For the proposed design, all cell parameters description and values will be described in Table 2. The geometry of metamaterial UWB antenna is presented in Fig. 11.

Table 2: Parameters description and values of unit cell I.

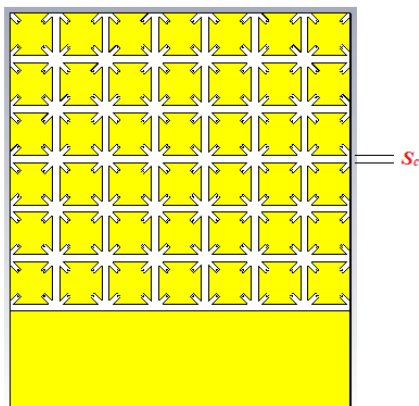| Parameter	Description	Value (mm)
C	Width of cell type I	3.5
l_m	Length of first slot	1.1
w_m	Width of first slot	0.4
l_r	Length of second slot	0.1
w_r	Width of second slot	0.2
S_c	Space between cells	0.5

Figure 11 The design of metamaterial antenna using cell type I on ground plane

Fig. 12, represents the return loss of the proposed antenna after adding Cell I to the ground plane.
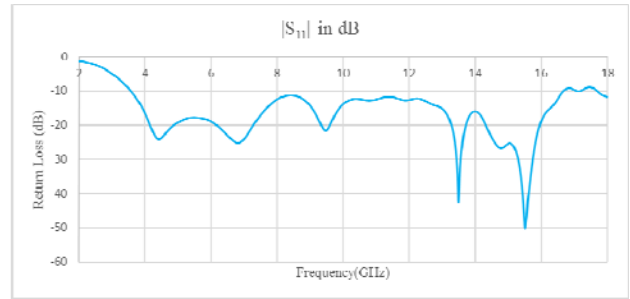

Figure 12 Return loss of the proposed antenna after adding Cell I

It is clearly shown from Fig. 12 that the bandwidth shows increasing in the higher frequency f_H and reaching the 16 GHz after adding the metamaterial to the ground plane which and the bandwidth enhancement is guaranteed for (3.7 – 16-5) GHz.

IV. IMPROVING ANTENNA BANDWIDTH USING METAMATERIAL CELL TYPE II

Second type of metamaterial unit cell was added to the patch and the ground plane. The return loss and VSWR results were calculated to illustrate the effect of cell II on enhancing the bandwidth especially in the higher frequency f_H. Fig. 13 shows the cell II geometry and parameters. In addition, Table 3, gives the cell II parameter description and initial value.
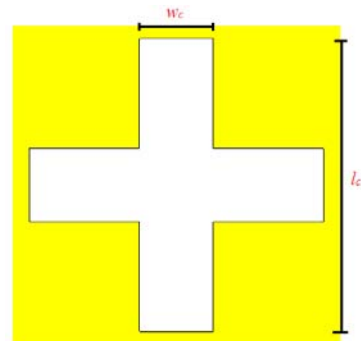

Figure 13 Unit cell type II geometry

Table 3: Unit cell II parameters description and value.

Parameter	Description	Value (mm)
l_c	Length of unit cell II	2.7
w_c	Width of unit cell II	0.75

The metamaterial unit cell type II was added in a geometrical shape as an array of six unit cells to the patch plane and another six cells to the ground plane. Fig. 14 shows the geometry and parameters of the proposed antenna after adding the metamaterial cell type I and II to the UWB antenna.
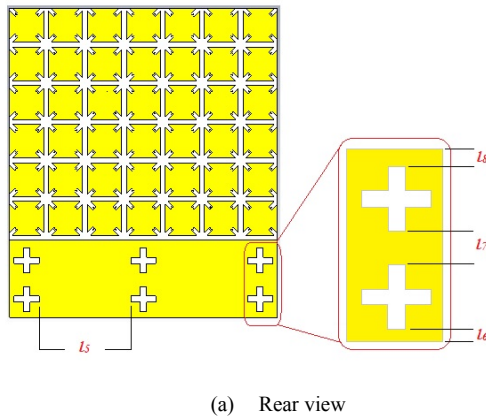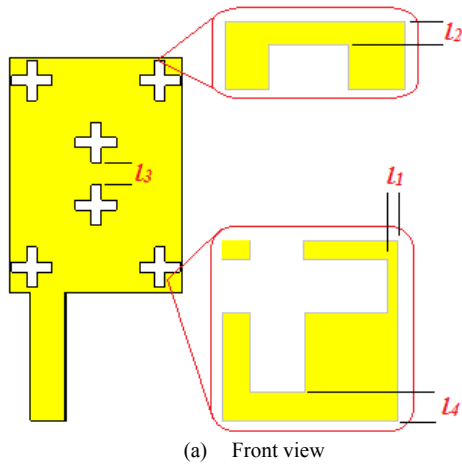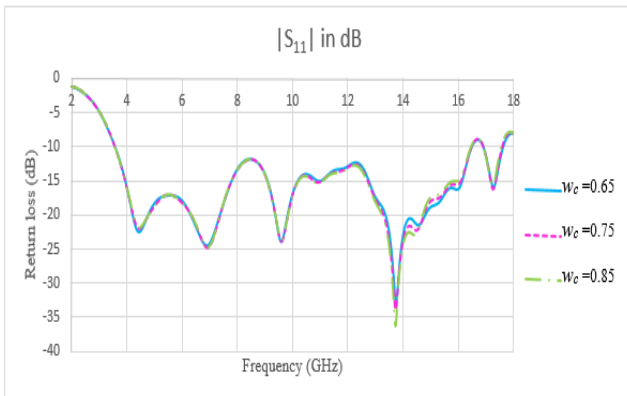
(a)   Front view

(a)   Rear view

Figure 14 Geometry of the proposed antenna with cell I and II
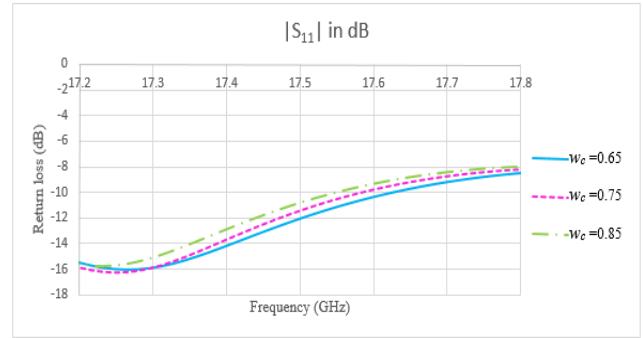
(a) Front view (b) Rear view.

After adding the metamaterial unit cell type II to both patch and ground, we will test the effect of changing the length and the width of the cell in increasing the bandwidth.

A- Variation of w_c

Fig. 15 shows the return loss response of the antenna for different values of w_c. It can be seen that the increasing of wc will decrease the higher frequency f_H.

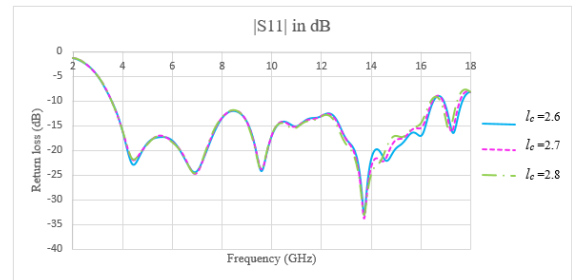(a)   Return loss for different values of (w_c) for the frequency range (2-18 GHz).

(b)   Return loss for different values of (w_c) for the frequency range (17.2-17.8 GHz).
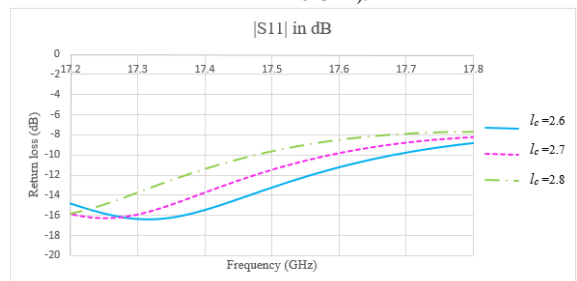
Figure 15 Return loss for different values of W_c.

B- Variation of l_c

Fig. 16 shows the return loss response of the antenna for different values of lc. It is obvious that the increasing of lc will decrease the higher frequency fH.

(a)   Return loss for different values of (l_c) for the frequency range (2-18 GHz).

(b)   Return loss for different values of (w_c) for the frequency range (17.2-17.8 GHz).

Figure 16 Return loss for different values of l_c.

V. OPTIMIZATION, SIMULATION, AND IMPLEMENTATION

Particle Swarm Optimization (PSO) is a mathematical method that is used to optimize a problem in a numerical and statistical procedure by trying a large number of iterations of the candidate parameter to improve it with respect to a given quality. PSO optimizes a problem by taking a population of candidate particles and moving these particles around in space of search according to simple mathematical methods over the position and velocity of this particle. Each movement is affected by its local best-known position and it is directed toward the best-known positions in the space of search. These particles update their position when they find that there is improvement in the value.

As expected, the parallel PSO algorithm optimizes the return loss (S11) of the designed antennas and improves antenna bandwidth. The PSO tries to find the optimum performance for the design that has below the threshold value given in the fitness function which is the return loss should be less than -10 dB. Table 4 represents the optimum values for the design.

Table 4: Optimum value of the design.

Parameter	Value (mm)
l_1	0.1248
l_2	0.138125
l_3	1.20125
l_4	0.336875
l_5	12.732836
l_6	0.600625
l_7	1.40012
l_8	0.799375
l_m	0.558614
w_m	0.403333
l_r	0.20166667
w_r	0.10916667

The electromagnetic performance of the optimized antenna is simulated using the electromagnetic CST MWS simulator.
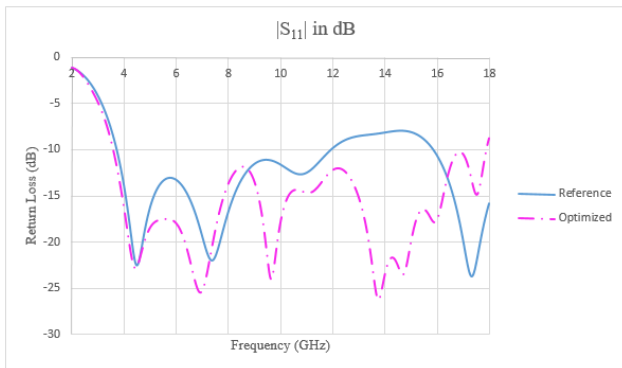

Fig. 17 The return loss responses of the reference and optimized design

Fig. 17 shows the return loss characteristics for the optimized antennas in comparison with the return loss for the reference antenna. The bandwidth of the reference antenna is 8.32 GHz (3.616-11.936 GHz), and for optimized antenna is 14.315 GHz (3.58-17.895 GHz). From below graph, it is obvious that the optimized design has achieved an enhancement in the bandwidth about 42% of its value after adding the metamaterial cells.

In addition, Fig. 18 and Fig. 19 represent the VSWR and gain response of the optimized design.
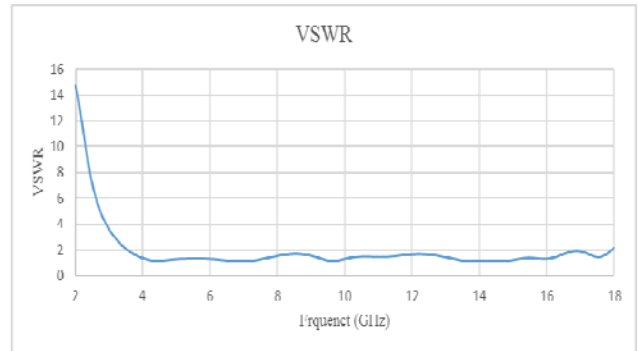

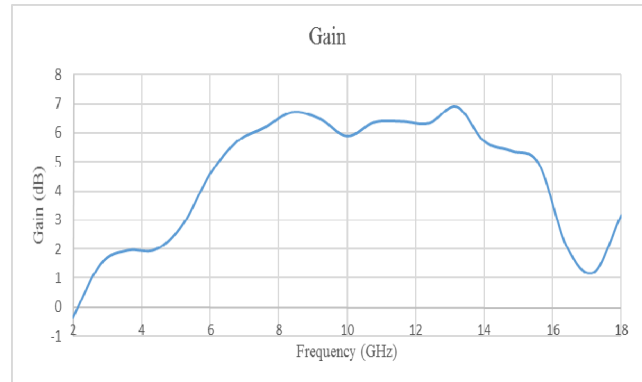Figure 18 VSWR response of the optimized design.

Figure 19 Gain response of the optimized design.

Implementation of the optimized antennas had been carried using PCB laser printer available in Jaavin Electronic Solution Company / Kuala Lumpur, Malaysia. The photographs of the antenna prototype are shown in Fig. 20.
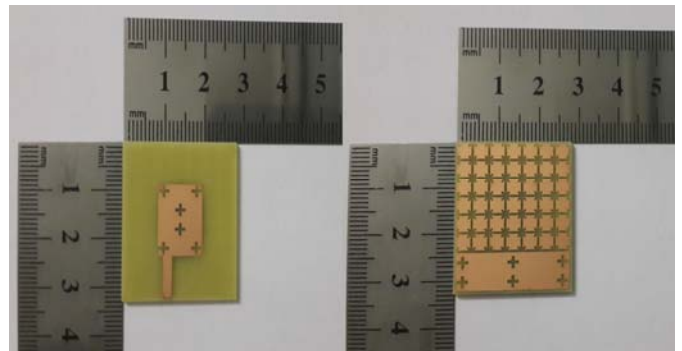

Figure 20 The prototype antenna.

After the construction, the characteristic measurements were performed using Vector Network Analyser (VNA-MS4642A). The return loss and input impedance versus frequency were measured. In addition, Fig. 21 shows the return loss of the fabricated antenna in comparison with the simulated antenna.
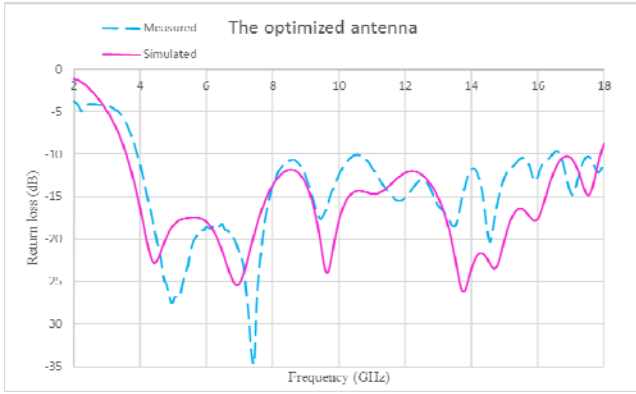
Figure 21: the measured and simulated return loss response.

Another important characteristic that is used to indicate whether the UWB pulse will be transmitted well or not, and to what degree it may be distorted or dispersed is the Group delay. If the phase is linear throughout the frequency range, the group delay will be constant for that frequency range. This linear phase and low dispersion guarantee low values of group delay, which are vital for transmitting and receiving a pulse with minimal distortion.

From the Fig. 22, it can be seen that the group delay is less than 1 ns in almost all the range of frequencies.
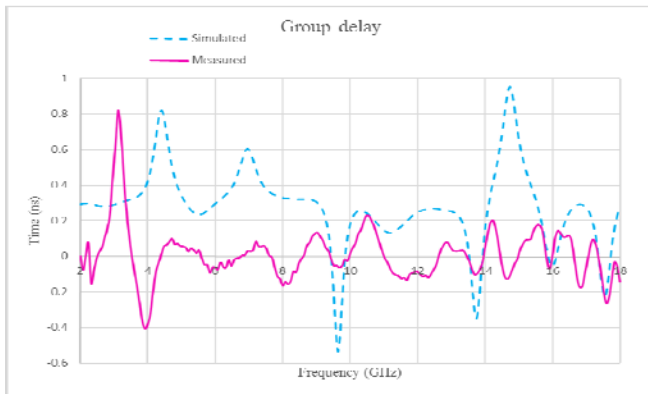

Figure 22: Group delay for simulated and measured results.

VI. CONCLUSION

In this work, an UWB metamaterial antenna has been designed, simulated, and implemented on a range of frequency from 3.58 GHz to 17.895 GHz. The purpose of this design is to illustrate the effect of adding the metamaterial cells in special shapes and types on the bandwidth enhancement of any UWB microstrip antenna. The resulting antenna has the advantage of reduced

dimensions (32 mm × 27.5 mm) and a bandwidth larger than that required by the standard FCC UWB. The conventional UWB metamaterial antenna is altered to enhance its specifications and produce a super wideband frequency range which can be used for different UWB applications.

The design has been optimized and verified using CST MW software package and it has been fabricated and tested successfully. The measurements of the fabricated antenna are almost similar to the simulation results but they are not typically the same due to the limited ability of the fabrication facilities.

Finally, the group delay of the antenna has an acceptable range, which is less than one ns, and that fits the UWB applications. The low values of group delay will ensure low distortion and low dispersion. With all features mentioned above, the proposed antenna seems to be attractive choice for many UWB communication applications.

REFERENCES

[1] Powell, J. "Antenna Design for Ultra-Wideband Radio", New Mexico State University, 2001.
[2] Randhawa, H. K. S. "Coplanar Waveguide Fed UWB Antenna with Dual Band Notch Characteristics", Thapar University, 2012.
[3] Hung-Jui Lam, "Ultra-Wideband Antenna in Coplanar Technology", University of Victoria, 2005.
[4] Bengal, W. "Microstrip Patch Antenna's Limitation and Some Remedies", International Journal of Electronic & Communication Technology, 2013.
[5] Eleftheriades, G. V. "EM Transmission-Line Metamaterials". Materials Today, 12(3), 30–41, 2009.
[6] Alù, A., & Engheta, N. "Guided Modes in a Waveguide Filled with a Pair of Single-Negative (SNG), Double-Negative (DNG), and/or Double-Positive (DPS) Layers". IEEE Transactions on Microwave Theory and Techniques, 2004.
[7] J. B, P., a.J, H., W.J, S., & Youngs I. "Extremely Low Frequency Plasmons in Metallic Microstructure", Imperial College London, 1996.
[8] Smith, D. R., Smith, D. R., Padilla, W. J., Padilla, W. J., Vier, D. C., Vier, D. C., … Schultz, S. "Composite Medium with Simultaneously Negative Permeability and Permittivity". Physical Review Letters, 2002.